Journal of Electron Spectroscopy and Related Phenomena, 54/55 (1990) 265–280
Elsevier Science Publishers B.V., Amsterdam

Vibrational Spectroscopy of Rare Gas Adlayers

Peter Zeppenfeld†, Ulrich Becher, Klaus Kern, and George Comsa

Institut für Grenzflächenforschung und Vakuumphysik, KFA Forschungszentrum Jülich, Postfach 1913, 5170 Jülich, Germany

†present address: IBM Almaden Research Center, 650 Harry Road, San Jose, CA 95120-6099

Abstract

An overview of the state of the art of the vibrational spectroscopy of physisorbed rare gas adlayers is given and some recent developments in this field are reported. High resolution thermal He atom scattering offers a unique means of probing low energy surface phonons. At present, an overall energy resolution of typically 0.3 meV can be achieved at a primary He beam energy of about 18 meV. This allows the rare gas adlayer vibration energies of the order of a few meV to be measured with high accuracy. In addition, small perturbations of the phonon dispersion and linewidth broadening originating from the coupling of the adlayer vibrations to the substrate phonons can be accessed. Recently, the effects of anharmonicity in thin rare gas films have been revealed by studying the temperature dependence of the phonon linewidths.
At the same time, the theoretical modeling of the dynamics of physisorbed adlayers has also evolved considerably. In its most advanced form, the theory uses realistic rare gas pair potentials, includes the dynamical coupling between the adlayer and the substrate, and takes into account anharmonic coupling terms between the rare gas atoms within the adlayer. As a result, an overall quantitative agreement between experiment and theory is obtained in the case of the rare gases Ar, Kr, and Xe physisorbed on Pt(111).

1. INTRODUCTION

Rare gas atoms may physisorb on graphite and various metal surfaces forming mono-, bi-, and trilayers, or films consisting of several tens of atomic layers. Such rare gas adlayers have attracted considerable interest during the last fifteen years because of their rich and subtle structural and dynamical properties. In the 1970's, the pioneering volumetric and thermodynamic measurements of the adsorption of rare gases on graphite powder substrates[1] were carried out, elucidating the adsorption properties and the thermodynamics of rare gas adlayers and thin films. These and similar experiments made a major contribution to the understanding of thin film growth and wetting phenomena[2]. Shortly thereafter the first diffraction studies of physisorbed rare gas adlayers[3] initiated a series of investigations uncovering the variety of quasi two dimensional structures such as the commensurate, incommensurate and high-order commensurate phases and the corresponding phase transitions. Neutron and X-ray diffraction have been used in con-

0368-2048/90/$03.50 © 1990 — Elsevier Science Publishers B.V.

junction with exfoliated graphite as a support, taking advantage of its high surface to volume ratio. Other, intrinsically surface sensitive, techniques such as *L*ow *E*nergy *E*lectron *D*iffraction (LEED) and thermal He atom scattering as well as X-ray diffraction at glancing incidence also allow *single crystal* graphite and metal surfaces to be used as a substrate. Ref. 4 lists some examples of recent investigations on the structure of physisorbed adlayers involving the different experimental techniques mentioned above.
Along with the experimental results there has been substantial theoretical effort dealing with the physics of physisorption[5], wetting[6], and structural 2D phase transitions[7]. The long standing fundamental interest in two dimensional systems was roused by the challenge of understanding the rare gas adlayers which in many respects may be considered to be a physical realization of two dimensional matter. Therefore the rare gas adlayers constitute a touchstone for the concepts and theories applying to systems with reduced dimensionality.

In addition to their structural properties, the dynamical behavior of the rare gas adlayers has been studied during the last five years. The first adlayer phonon was measured by Mason and Williams[8] for Xe on Cu(110) and Gibson et al.[9] reported the first measurement of complete phonon dispersion curves of 1, 2, 3 and 25 layer thick rare gas films physisorbed on the Ag(111) surface. They were able to resolve the phonon energies as small as a few meV using inelastic thermal He atom scattering. This technique continues to be the most commonly used in the experimental investigation of the lattice dynamics of thin physisorbed rare gas films. Therefore, we will give a brief description of the method and its application to physisorbed systems in section 2.
As for the early measurements of the lattice dynamics of Ar, Kr, Xe on Ag(111)[9] and Xe on Pt(111)[10], the dispersion curves could be accounted for nicely by a simple lattice dynamical calculation in which the substrate is assumed to be rigid, serving only to bind the adlayer with a force constant which matches the measured frequency of the monolayer-substrate perpendicular vibration mode. These studies demonstrate in an instructive way how the adlayer vibration mode gradually evolves from a dispersionless Einstein mode for the monolayer towards a surface Rayleigh wave, characteristic of a semi-infinite crystal, in the 25 monolayer films. This evolution of the lattice dynamics with increasing film thickness will be discussed in section 3.
Despite the general agreement of the simple rigid substrate approximation and the measured dispersion curves, an anomalous variation of the phonon linewidth with phonon wavevector together with a modulation of the measured inelastic He signal along the Brillouin zone was observed[9] and tentatively attributed to the dynamical coupling of the adlayer to the underlying Ag(111) substrate. A subsequent theoretical study by Hall, Mills, and Black[11] explored the possible effects of such a dynamical coupling on the adlayer phonon dispersion and linewidths. In this calculation the substrate was no longer assumed to be rigid, but was instead approximated by an elastic continuum. As a result, the authors predicted three mechanisms through which a dynamical coupling would manifest itself: a hybridization (avoided crossing) of the adlayer vibration mode and the substrate Rayleigh wave, a linewidth broadening of the adlayer phonons due to the coupling to the substrate bulk phonons, and another avoided crossing between the adlayer mode and the substrate longitudinal bulk band edge. In section 4 we will discuss these effects in depth

and we will demonstrate how the theoretical predictions have been verified in every detail by recent experiments[12-14].
Exploring further aspects of the dynamical behavior of rare gas adlayers we have performed temperature dependent measurements of the adlayer phonon linewidths[15]. A significant increase of the phonon linewidths with temperature has been observed, demonstrating the contribution of the anharmonicity of the coupling between the rare gas atoms in the adlayer. These measurements are presented in section 5 together with the most recent and refined theoretical description[13,15] of the dynamical behavior of rare gas adlayers physisorbed on Pt(111). This description uses the well known rare gas pair potentials to extract the force constants and anharmonic coupling terms between the rare gas atoms. It further includes the coupling of the adlayer to the substrate, treating the Pt(111) substrate as an elastic continuum. With a single empirical constant tuning the strength of the coupling to the substrate, a satisfying overall quantitative agreement with the experimental data is achieved.
Finally, section 6 addresses the question of how the vibrational spectroscopy can actually be used as a tool in investigating structural and kinetic properties. Some examples of recent efforts in this area are presented and an outlook on possible future applications of the vibrational spectroscopy of physisorbed adlayers is given.

2. EXPERIMENTAL

Compared to most chemically bound adsorbates, the binding of the rare gas atoms to crystal surfaces is very weak (<300 meV). Besides the physisorption potential being very shallow it is also quite flat and the associated vibration frequency is low. This imposes two main criteria to be met by any experimental technique probing the lattice dynamics of rare gas adlayers: the technique has to be non-destructive in order not to destroy the weakly bound physisorbed adlayer; at the same time the energy resolution must be high enough to resolve the details of the phonon spectrum (<1 meV). *H*igh *R*esolution *E*lectron *E*nergy *L*oss *S*pectroscopy (HREELS) currently barely provides the desired energy resolution. Thermal neutron scattering is non-destructive and the required energy resolution is easily achieved; however, neutrons are not sensitive to surfaces and can therefore be used only in connection with a few selected substrates with high surface to volume ratio, namely graphite and MgO(100) powders. Furthermore, the broad distribution of the orientation of the individual microcrystallites in these substrates generally leads to an averaging of the information; thus the extraction of specific lattice dynamical data such as the phonon energy as a function of the 2D wavevector can be extremely difficult. The only method so far that combines surface sensitivity, high energy resolution and non-destructiveness is the (inelastic) scattering of thermal He atoms.

The basic capabilities of thermal He atom scattering already became apparent from the work of Otto Stern's group in the early 1930's[16]. However, it was only after the introduction of nozzle beams that He scattering became a powerful and efficient tool for surface investigations. Compared to classic effusive Knudsen cells, nozzle beam sources achieve a simultaneous increase of both the intensity *and* the monochromaticity of the beam[17].

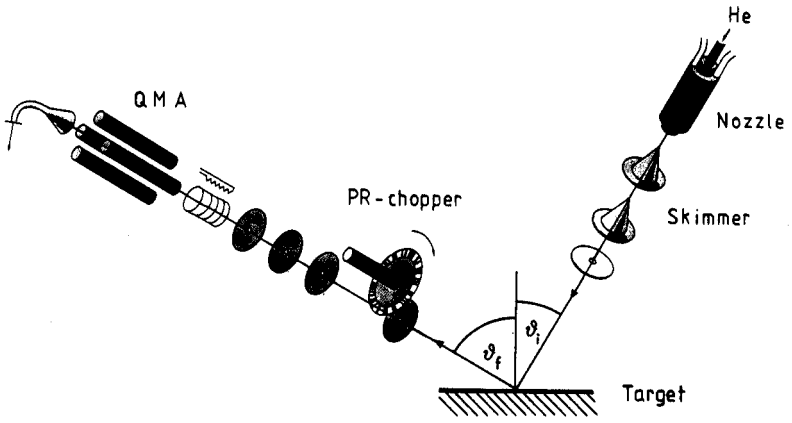

Figure 1: Sketch of a He scattering experiment. From right to left: He nozzle, target (scattering angles ϑ_i and ϑ_f), pseudorandom (PR) chopper, and quadrupole mass analyzer (QMA).

During the past ten years numerous applications of the He scattering technique to the study of adsorption[18], structure[19], and dynamics[20] on surfaces have been reported.

A typical He scattering apparatus as sketched in figure 1 consists of a He nozzle source, a UHV scattering chamber hosting the sample along with the standard surface analytical tools (Auger, LEED, sputtering gun, etc.), and a He atom detector - usually a mass filter. In inelastic scattering experiments a time-of-flight (TOF) analysis is performed in order to determine the energy of the scattered He atoms. For this purpose, the He beam is mechanically chopped and the time needed for the atoms to reach the detector is measured. From the time-of-flight and the known length of the flight path the (kinetic) energy of the He atoms is obtained.

The particular experimental setup we have been using for our experiments on the rare gas adlayer dynamics is described in ref. 21. The He nozzle source generates a He beam with an intensity of about 10^{19} He atoms/(sterad sec) collimated to 10^{-6} sterad and with an energy spread of $\Delta E/E = 1.4\%$. We use the pseudorandom chopping technique[21,22] to achieve a high time resolution (2.5 μs over a flight path of 790 mm) without reducing the transmission of the TOF-spectrometer. Together with the energy spread of the incoming He beam an overall energy resolution of 0.32 meV at a primary He beam energy of 18.3 meV is obtained. The total scattering geometry being fixed, the incoming beam and the He beam reaching the detector make a constant angle $\vartheta_i + \vartheta_f = 90°$. The scattering conditions are varied by rotating the crystal in the scattering plane changing ϑ_i and ϑ_f simultaneously. The angular divergence of both the incoming and outgoing beam is 0.2°, translating into a wavevector resolution of about 0.02 Å^{-1} at a typical He energy of 18 meV.

From the measured He energy loss ($\Delta E < 0$) or gain ($\Delta E > 0$) the phonon energy $\hbar\omega$ and the corresponding phonon wavevector $\vec{Q}$ parallel to the surface is straightforwardly determined from the conservation of energy $\Delta E = E_f - E_i = \hbar\omega$ and parallel wavevector $\Delta\vec{K} = \vec{K}_f - \vec{K}_i = \vec{Q}$. In the case of in plane scattering the relation between energy and momentum transfer is then given by the *scancurve*

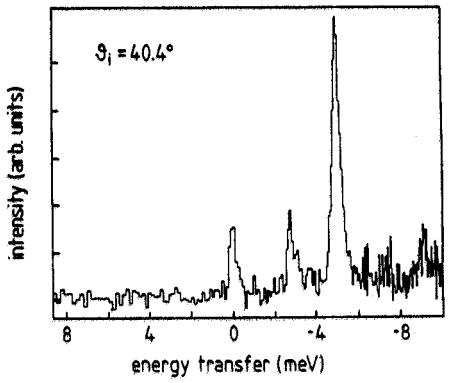

Figure 2: He TOF spectrum of an Ar monolayer on Pt(111) taken at an angle of incidence $\vartheta_i = 40.4°$ along the $\overline{\Gamma M}$ direction; surface temperature $T = 25$ K; primary He beam energy $E_i = 18.3$ meV [14].

$$\Delta E = E_i \left[\left(\frac{\sin \vartheta_i + \Delta K/k_i}{\sin \vartheta_f} \right)^2 - 1 \right] \tag{1}$$

where $k_i = \sqrt{2m_{He}E_i}/\hbar$ denotes the wavevector of the incoming He atoms. As an example, figure 2 shows an inelastic He scattering spectrum from a monolayer of Ar on Pt(111) obtained with a primary He beam energy of 18.3 meV at a scattering angle $\vartheta_i = 90° - \vartheta_f = 40.4°$ along the $\overline{\Gamma M}$ symmetry direction of the Ar layer (corresponding to the $[11\bar{2}]$-direction in real space). The small peak at zero energy transfer represents the purely elastically scattered He atoms. Away from the position of the Bragg-peaks of the overlayer, the intensity of this diffuse elastic peak is a sensitive measure of the perfection and cleanliness of the surface. The main peak at -5.0 meV ($Q = 0.0$ Å^{-1}), corresponds to the creation of an Ar monolayer phonon associated with the vertical Ar-Pt vibration. A second inelastic feature is observed at -2.9 meV ($Q = 0.3$ Å^{-1}). As will become clear in section 4, this feature is related to the Pt Rayleigh wave and originates from the dynamical coupling of the adlayer and the Pt(111) substrate.

The sample used in the experiments reported below is a high quality Pt(111) single crystal with an average terrace width > 2000 Å [23]. The rare gas adlayers are deposited by exposing the clean Pt(111) surface at ~ 20 K to a 3D rare gas atmosphere (between 10^{-9} and 10^{-7} mbar) and pumping off the rare gas pressure when the desired coverage is reached. By a procedure outlined below and described in ref. 10 the exposure needed for the completion of successive layers can be determined to within a few percent.

3. LATTICE DYNAMICS AS A FUNCTION OF FILM THICKNESS

A perfect two dimensional layer, consisting of atoms arranged periodically in a primitive 2D Bravais lattice and elastically coupled to each other, exhibits two vibration modes, both involving lateral displacements of the atoms within the layer. Along directions of high

symmetry (where the wavevector of the phonon lies in a mirror plane of the layer) these two modes are orthogonally polarized in the direction of propagation (longitudinal mode) and the perpendicular direction in the plane (transverse mode), respectively. The dispersion of the vibration modes is easily obtained from a calculation similar to the one dimensional "linear chain" problem treated in most standard textbooks on solid state physics. For instance, in the case of a hexagonal 2D lattice, assuming a coupling ϕ'' between nearest neighbor atoms only, and with the phonon wavevector Q along the $\overline{\Gamma M}$-direction, the two modes are given by: $\omega_L = \sqrt{6\phi''/M}\ \sin(Q\sqrt{3}\,a/4)$ and $\omega_T = \sqrt{2\phi''/M}\ \sin(Q\sqrt{3}\,a/4)$. Here ω_L and ω_T denote the vibration frequencies of the longitudinal (L) and the transverse (T) mode, respectively; M is the mass of the atoms within the layer and a the nearest neighbor distance. $\omega(Q)$ is called the *dispersion relation* of the mode. Upon "pinning" the 2D layer onto a substrate, a third vibration mode ($\perp$) connected with the vibration of the adlayer atoms with respect to the underlying substrate is introduced. If the substrate is assumed to be smooth and rigid, and the corresponding force constant ϕ_0'' acting in the direction normal to the surface, the perpendicular mode $\perp$ is characterized by a single vibration frequency $\omega = \sqrt{\phi_0''/M}$ independent of the wavevector Q parallel to the surface. This dispersionless vibration mode is commonly refered to as an *Einstein mode*. The situation of a 2D (hexagonal) layer pinned to a substrate corresponds to the case of a rare gas monolayer adsorbed on graphite or a fcc(111) metal surface. In fact, to a first approximation the perpendicularly polarized $\perp$-mode as measured with inelastic He scattering for various monolayer rare gas systems[9,10,12] is nearly dispersionless. Because in plane scattering is not sensitive to the purely transverse modes, and since He scattering predominantly probes the perpendicularly polarized modes, there is so far no direct experimental information on the dispersion of the purely transverse and longitudinal vibration modes of rare gas films.

Upon adsorption of a second layer on top of and in registry with the monolayer the number of phonon branches increases by another three modes. In addition, the coupling between the first and second layer is no longer directed perpendicular to the surface (assuming a fcc or hcp stacking and central forces). This leads to a mixture between perpendicular and longitudinal polarization creating so called *sagittally* polarized modes. Along the high symmetry directions these sagittally polarized modes are still decoupled from the orthogonally polarized transverse modes. In the case of a bilayer there are thus 4 sagittal and 2 transverse vibration modes. The coupling of the longitudinal and perpendicular displacements of the adlayer atoms also introduces a dispersion of the mainly perpendicularly polarized modes seen in inelastic He scattering. The adsorption of further layers again adds more branches to the vibration spectrum and leads to an increased dispersion of the strongly perpendicularly polarized modes. Finally, at large film thickness the surface main vibration mode approaches the Rayleigh wave, characteristic of the semi-infinite rare gas (111) crystal[9,10]. The change of the dynamical behavior is most prominent at small wavevector Q: since the monolayer Einstein mode is an optical, dispersionless mode and the Rayleigh wave an acoustical, sinusoidal mode, the vibration frequency at the $\overline{\Gamma}$-point ($Q = 0$) has to drop from its maximum value in the monolayer to zero as the film thickness is increased. Thus, the phonon energy "gap" at the center of the Brillouin zone, $Q = 0$, is a direct measure of the finite thickness of the adsorbed film. Figure 3 shows a series of He energy spectra taken from Xe adlayers of various thickness

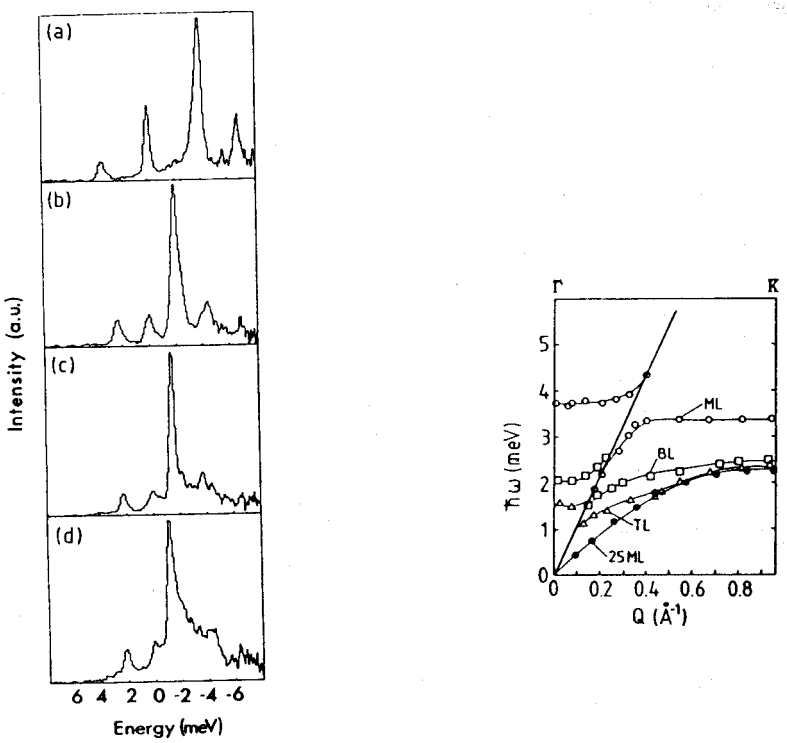

Figure 3: Left: He TOF spectra taken from a Xe ML (a) BL (b), TL (c), and 25 layer thick film (d) on Pt(111). The scattering conditions are the same for all spectra ($\vartheta_i = 42°$ along the $\overline{\Gamma M}$ direction of the Xe film; primary He beam energy $E_i = 18.3$ meV); surface temperature $T = 25$ K.
Right: Xe/Pt(111) dispersion curves. Besides the evolution of the dispersion curves with increasing film thickness, the hybridization of the adlayer mode and the Pt(111) Rayleigh wave is apparent (see section 4).

physisorbed on Pt(111). The spectra were obtained under identical scattering conditions. It is evident from the spectra that the position of the main inelastic peak is displaced to smaller loss energies as the film thickness is increased. It is important to note, that the shift of the peak position is not continuous: a film of nominally 1.5 layers yields an energy spectrum which is the weighted sum of the monolayer (ML) and the bilayer (BL) spectrum rather than showing a single loss peak at an intermediate energy. This means that the growth of the multilayer films indeed proceeds in a layer-by-layer mode. On the other hand, the fact that the next layer phonon emerges at a discrete, characteristic energy as soon as the previous layer is completed can be used to calibrate the rare gas dose needed for completion of successive layers[10]. This procedure allows the adlayers to be grown to the nominal thickness with an accuracy of a few percent of a monolayer up to the 4 to 5 ML films. Then the energy difference between the phonons associated with films differing by a single layer in thickness becomes too small to be experimentally resolved. Since the rare gas dose per newly added atomic layer does not change signif-

icantly beyond the trilayer, the rare gas dose corresponding to films thicker than about five monolayers can be safely extrapolated.
The dependence of the dynamical behavior on the thickness of the physisorbed rare gas films is illustrated even more impressively by the variation of the layer specific phonon dispersion curves, also shown in figure 3. These curves were obtained from a large number of individual spectra taken at different angles of incidence ϑ_i, corresponding to different parallel wavevector Q. As anticipated from the discussion above, the dispersion of the mainly perpendicular surface mode changes from a nearly dispersionless behavior of the monolayer to the characteristics of the Rayleigh wave for the 25 ML film. Note however, that there is a strong anomaly in the dispersion of the adlayer mode where it intersects the Rayleigh wave of the Pt substrate, indicated by the dark solid line in the dispersion plot in figure 3. Obviously, we have to take into account the dynamics of the underlying Pt substrate in order to understand this more complex behavior of the combined rare gas adlayer-substrate physisorption system.

4. THE ADLAYER-SUBSTRATE DYNAMICAL COUPLING

As mentioned in the introduction, the shortcomings of the simple rigid substrate approximation already became apparent in the early measurements of the lattice dynamics of the rare gas adlayers physisorbed on Ag(111)[9]. However, the evidence was indirect and the phonon dispersion itself did not seem to be affected within the accuracy of the available experimental resolution. In response to the first measurements, Hall, Mills, and Black[11] evaluated the possible effects of a dynamical coupling between adlayer and substrate on the adlayer phonon dispersion assuming an elastic continuum as a substrate. They predicted a hybridization of the adlayer mode and the substrate Rayleigh wave resulting in an avoided crossing of the modes associated with an energy splitting of the order of 0.5 to 1 meV. Such an avoided crossing was also inferred earlier from a slab calculation of the lattice dynamics of a Xe monolayer on Gr(0001)[24]. Besides the avoided crossing with the Rayleigh wave Hall et al. predicted a coupling mechanism of the adlayer mode to the substrate bulk phonons: in the wavevector region where the adlayer mode overlaps the substrate bulk phonon bands, the transfer of the adlayer vibration energy into the substrate bulk via the excitation of bulk phonons will lead to a shortening of the adlayer phonon lifetime, resulting in a measurable energy broadening of the phonon linewidth of a few tens of a meV. This coupling mechanism was named "radiative damping". Even the details of the density of states of the bulk substrate phonons should be reflected in the dynamical coupling. In particular another (though smaller) avoided crossing of the adlayer mode and the longitudinal bulk band edge of the substrate is expected as a consequence of the van Hove singularity $(\omega - c_l Q)^{-1/2}$ of the bulk density of states.

Recently these theoretical predictions have been verified experimentally for the rare gas adlayers physisorbed on Pt(111)[12-14]. Partial evidence for the dynamical coupling between adlayer and substrate has also been obtained for the rare gases on Ag(111)[25] and Xe on graphite[26]. Figure 4 shows a series of He TOF spectra from an Ar monolayer physisorbed on the Pt(111) surface while figure 5 displays the phonon dispersion curve together with the phonon linewidths obtained from a large number of such spectra. These data nicely

demonstrate the influence of the substrate on the adlayer phonon linewidth and dispersion. Due to the small energy of the Ar-Pt vibration of about 5 meV the Ar adlayer mode lies well below the substrate vibration modes at larger wavevectors Q. In this region no vibrational coupling to the substrate is expected to occur. As an example, the inelastic feature in spectrum (d) of figure 4 corresponds to the creation of an Ar adlayer phonon of -4.8 meV with wavevector $Q = 0.78$ Å^{-1}, i.e. close to the zone boundary $Q(\overline{M}) = 0.98$ Å^{-1}. The observed narrow linewidth is solely determined by the instrumental resolution $\Delta E_{instr} = 0.32$ meV of our spectrometer. Closer to the center of the Brillouin zone ($\overline{\Gamma}$), however, the adlayer mode overlaps the substrate bulk phonons (indicated by the hatched area in figure 5) and crosses the Pt-Rayleigh wave (solid line in figure 5) at $Q = 0.4 - 0.5$ Å^{-1}. As a consequence, the main loss peak in spectrum (a) ($Q = 0.0$ Å^{-1}) and (b) ($Q = 0.28$ Å^{-1}) is considerably broadened. In addition, a second inelastic feature is observed shifting from -2.9 meV at $Q \approx 0.3$ Å^{-1} in spectrum (a) towards the main peak with which it forms a doublet at $Q = 0.4 - 0.5$ Å^{-1} as evidenced in spectrum (c). The energy variation with phonon wavevector of this second inelastic feature coincides with the known dispersion of the Pt(111) Rayleigh wave[27]; the mere "visibility" of the Pt related vibration mode with inelastic He scattering which is known to probe only the topmost (Ar) layer is a direct manifestation of the vibrational coupling of the Ar monolayer to the underlying Pt-substrate. The increase in scattering intensity as the Pt-peak approaches the adlayer phonon peak, and the avoided crossing leading to an energy splitting of about 0.8 meV, are a clear demonstration of the hybridization of the two modes. The "radiative damping" resulting in a net linewidth broadening $\varepsilon \equiv [(\Delta E)^2 - (\Delta E_{instr})^2]^{1/2}$ of 0.2 to 0.3 meV close to the zone center, as well as the hybridization of the Ar adlayer mode and the Pt Rayleigh wave, are most obvious from figure 5, where we plot the phonon dispersion together with the linewidth broadening obtained from a large number of spectra like those in figure 4. Furthermore, a pronounced increase of the phonon linewidth in a narrow wavevector range from $Q = 0.2$ to 0.3 Å^{-1} is evident from figure 5. (Spectrum (b) in figure 4 shows a corresponding He energy spectrum.) The wavevector range where this extra

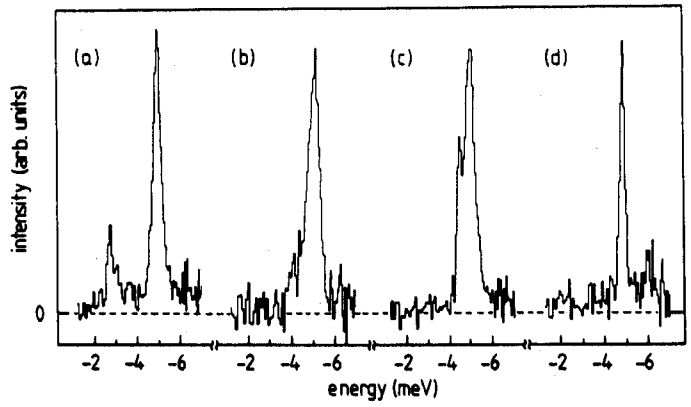

Figure 4: He TOF spectra taken from a monolayer of Ar on Pt(111). $E_i = 18.3$ meV; $T = 25$ K; (a) $\vartheta_i = 40.4°$, (b) $\vartheta_i = 38.5°$, (c) $\vartheta_i = 37.7°$, and (d) $\vartheta_i = 35.0°$ [14].

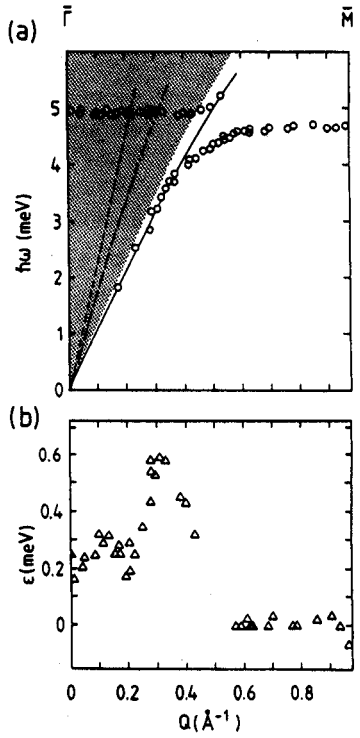

Figure 5: Dispersion curve (a) and reduced phonon linewidth ε (b) along the $\overline{\Gamma M}$ symmetry direction for monolayer Ar/Pt(111). The shaded area indicates the surface projected bulk phonon bands. Also indicated are the Pt Rayleigh wave (solid line), the longitudinal Pt bulk band edge (dashed line), and the longitudinal resonance (dash-dotted line)[14].

linewidth broadening is observed corresponds to the region where the adlayer mode crosses the longitudinal bulk band edge of the Pt substrate[27]. Therefore we may identify the extra broadening with the anomaly of the phonon dispersion due to the van Hove singularity of the bulk phonon density of states at the longitudinal bulk band edge. It should be pointed out that Hall, Mills, and Black expect a hybridization rather than a linewidth broadening. We believe that the expected hybridization is seen in the experimental data only as a broadening, because the energy splitting involved in the hybridization is so small ($\lesssim 0.3$ meV) that the present instrumental resolution along with the linewidth broadening due to the "radiative damping" does not allow the hybridization to be resolved experimentally. Similarly, the much larger phonon linewidths due to "radiative damping" in the Kr and Xe monolayers on Pt(111) (0.55 and 0.58 meV, respectively) as compared to the Ar/Pt(111) case might be the reason why an *extra* broadening due to the van Hove anomaly has not been observed experimentally for Kr or Xe[12,13].

As can be seen from figure 5, the wavevector range in which the van Hove anomaly is observed is shifted to slightly higher wavevector as expected from the crossing of the adlayer mode and the Pt bulk band edge (indicated by the dashed line in figure 5). A

possible explanation is given by the fact that on the Pt(111) surface a resonant mode peals off the longitudinal bulk band edge and gives rise to a surface branch ("longitudinal resonance") lying slightly below the bulk band edge (dash dotted line in figure 5). It seems plausible, that besides the coupling to the band edge, the adlayer mode is similarly affected by the enhanced surface density of states at this longitudinal resonance. Therefore the extra linewidth broadening is most likely due to the coupling of the adlayer mode to both the longitudinal bulk band edge *and* the surface longitudinal resonance.
In summary, the rare gas adlayers on Pt(111) - and in particular the Ar monolayer - present textbook-like examples of the dynamical coupling of a quasi two dimensional layer to an underlying elastic substrate.

5. ANHARMONIC EFFECTS ON THE RARE GAS ADLAYER VIBRATIONS

Another interesting finding came out of the experimental investigation of the phonon linewidths of the rare gas bi- and trilayers on Pt(111)[12,13]: At large wavevectors, well beyond the "radiative damping" cut-off, linewidths of about 0.2 meV were measured for the bi- and trilayer phonons, in contrast to the monolayer where the intrinsic linewidth was too small to be resolved (< 0.1 meV, see e.g. figure 5). Unlike the "radiative damping", this linewidth broadening cannot be explained by a direct coupling of the adlayer to the substrate. Since anharmonic effects are known to play an important role in the three dimensional rare gas systems, a possible source of this broadening might be the anharmonic interaction between the rare gas atoms themselves. Therefore, using a perturbation theory approach, Hall and Mills have explored whether the anharmonic interactions between the rare gas atoms can account for the observed linewidths in the bi- and trilayer[13]. In the anharmonic interaction picture, a damping leading to a linewidth broadening is produced by multi-phonon decay processes. In this calculation only the contribution to lowest order in perturbation theory (involving the interaction terms which are cubic in the relative displacements of the rare gas atoms) have been taken into account. Therefore, only three-phonon decay processes are considered; namely, the process in which a single phonon splits into a pair of new phonons and the complimentary process in which two phonons combine into a single one. While presenting the main contribution to the anharmonic broadening in the bi- and trilayers these processes do *not* affect the phonon linewidth in the monolayer system. Indeed, since the polarization vectors of the three monolayer vibration modes are mutually orthogonal to each other, and due to the simultaneous constraint of conservation of phonon energy and parallel momentum, the matrix element describing the three-phonon decay of a monolayer $\perp$-phonon exactly vanishes[13]. Therefore, only much weaker decay processes involving higher order coupling terms contribute to the monolayer phonon linewidths. As a result, the anharmonic coupling nicely accounts for the striking difference observed in the phonon linewidths of the monolayer and the multilayer systems. Beside this qualitative agreement, the calculated linewidths for the bi- and trilayer systems also quantitatively fit the experimental findings rather well. This is shown in figure 6 where the dispersion and the phonon linewidths for the Ar bi- and trilayer are plotted. The anharmonic contribution to the linewidth calculated assuming realistic rare gas pair potentials is indicated by the solid

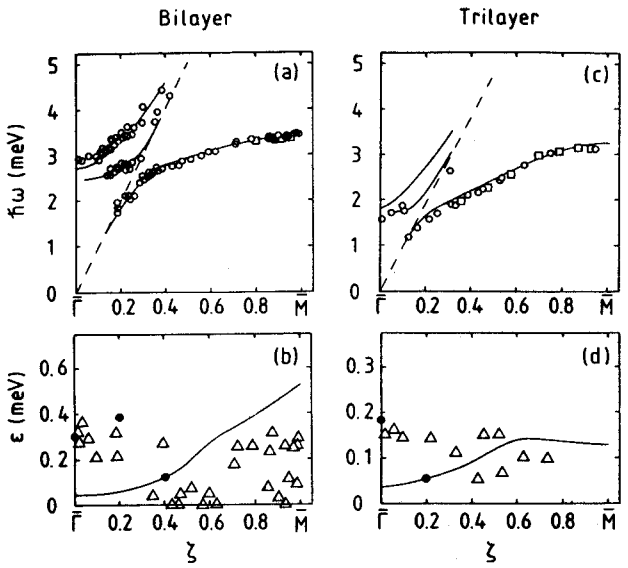

Figure 6: Comparison of the measured and calculated phonon dispersion and linewidths for the Ar bi- and trilayer on Pt(111) at $T = 25$ K. Open symbols are experimental data, the solid lines in the upper part indicate the calculated dispersion curves of the mainly perpendicularly polarized adlayer modes. The coupling to the Pt substrate has been included; the dashed line corresponds to the Pt(111) Rayleigh wave. In the lower part, the solid line indicates the calculated anharmonic linewidths, and the filled circles are total phonon linewidths where the "radiative damping" has been included.

line together with the experimental data points in the lower part of figure 6. Despite the relatively large scattering in the experimental data, the magnitude of about 0.3 meV for the Ar bilayer and 0.1 meV for the trilayer is fairly well reproduced, and the measured linewidths of the bilayer phonons even seem to follow the same increase with reduced wavevector $\zeta \equiv Q/Q(\overline{M})$ as the theoretical curve. For wavevectors Q below the "radiative damping" cut-off where the adlayer overlaps the Pt bulk phonons, the linewidths cannot be described by the anharmonic contribution alone. Indeed, the dynamical coupling of the adlayer to the Pt substrate does not only affect the monolayer, but extends to the bi- and trilayer films. Therefore, "radiative damping" is expected. In fact, including the coupling to the substrate in the elastic continuum approximation the total linewidths calculated for selected points in the Brillouin zone (solid circles in figure 6) are substantially larger in the overlap region and agree well with the experimental data. The upper part of figure 6 illustrates how the theoretical modeling of the lattice dynamics including the coupling to the surface nearly perfectly reproduces the measured bi- and trilayer Ar/Pt(111) dispersion curves. Note in particular that in the bi- and trilayer one still observes a significant hybridization of the adlayer modes with the Pt Rayleigh wave. A similar overall agreement between theory and experiments is also obtained for Kr and Xe adlayers on Pt(111)[13].

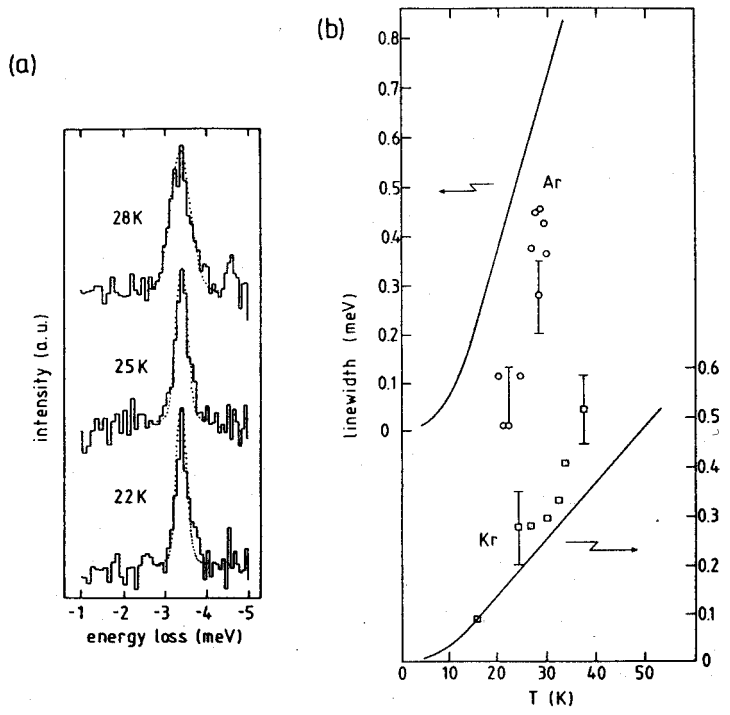

Figure 7: (a) He TOF spectra taken from an Ar bilayer on Pt(111) at different temperatures. $E_i = 18.3$ meV; $\vartheta_i = 35°$ with the scattering plane oriented along the $\overline{\Gamma}\overline{M}$-azimuth of the Ar bilayer. (b) Phonon linewidths at the zone boundary for an Ar and Kr bilayer on Pt(111) as a function of temperature. Circles refer to Ar (measured at the $\overline{M}$-point), squares to Kr (measured at the $\overline{K}$-point). The solid lines represent the theoretical temperature variation of the anharmonic phonon linewidth broadening evaluated to lowest order in perturbation theory[15].

As a further test of the role of anharmonicity in the adlayer dynamics, we have recently explored the temperature dependence of the linewidth of the rare gas adlayer phonons[15]. Figure 7a presents a series of He energy loss spectra from an Ar bilayer on Pt(111) at three different temperatures at an angle of incidence $\vartheta_i = 35°$, thus sampling the adlayer phonon close to the zone boundary at the $\overline{M}$-point. The spectra strikingly demonstrate the effect of the surface temperature on the linewidth: the phonon loss peak broadens substantially upon increasing the temperature from 22 to 28 K. (A further temperature increase results in the evaporation of the topmost layer of the bilayer Ar film.) Figure 7b displays the phonon linewidths for the Ar and Kr bilayer at the boundary of the Brillouin zone as a function of temperature. The solid lines indicate the corresponding anharmonic linewidth broadening calculated in lowest order perturbation theory as described above. Above 10 K the phonon linewidth is found to vary linearly with temperature as expected for processes involving only cubic terms of the rare gas interaction potential. Although the absolute values of the theoretical and measured linewidths differ by a factor

of 1.5 or so, the overall shape of the temperature dependence is similar. In particular, the two different slopes for Ar and Kr are well reproduced by theory. We may therefore conclude that the linewidth broadening of the rare gas adlayer phonons at the zone boundary is indeed dominated by anharmonic damping within the rare gas adlayer.

6. FURTHER APPLICATIONS AND FUTURE DEVELOPMENTS

Besides the understanding of the dynamical behavior of the rare gas adlayer itself, the vibrational spectroscopy of these systems can be used as an investigational tool. The vibrational spectroscopy applied to chemisorbed systems supplies information on adsorption sites, chemical nature, and reaction paths of chemisorbed species[28]. Similarly, the vibrational spectroscopy of physisorbed systems can provide valuable information on the structure, the growth mode, or the diffusion kinetics of these adlayers.
As an example, we have shown in section 3 that the phonon spectrum of a multilayer rare gas film is intimately related to the thickness of the film. Therefore thin film growth and wetting can be characterized by monitoring the adlayer lattice dynamics. In addition, two dimensional structures can be studied by probing the adlayer phonon modes: in the thin film, the phonon gap at the $\overline{\Gamma}$-point of the perpendicularly polarized vibration mode is determined by the finite extension of the film in the direction normal to the surface. Similarly, a *commensurate* 2D adlayer structure, which can be mapped onto a finite unit cell on the substrate also leads to a phonon gap in the adlayer modes. Since in this case the confinement is along the directions parallel to the surface, only the laterally polarized longitudinal and the transverse modes are affected. On the other hand, a truly *incommensurate* (floating) phase is characterized by an undisturbed acoustic dispersion of the longitudinal and transverse phonon branch. Thus the phonon gap in the dispersion of the longitudinal mode could be used in principle to distinguish commensurate or locked phases from incommensurate structures. Unfortunately, He scattering experiments have not succeeded in measuring the purely longitudinal monolayer phonons, yet. Since the inelastic He scattering cross section for longitudinal modes is strongly enhanced for large wavevector transfer, this problem may be overcome when He scattering experiments at large total scattering angle $\vartheta_i + \vartheta_f$ are carried out. Until recently, the accessible scattering angles in most He scattering experiments were limited by instrumental design. However, inelastic neutron measurements have resolved the longitudinal phonons of Ar on graphite[29] and recently the observation of the phonon gap in a commensurate physisorbed D_2-layer was reported[30]. Yet the neutron scattering signal only gives averaged information and the possibility to probe the longitudinal dispersion curves with He scattering would be of great importance.

Another interesting application is concerned with disordered or weakly ordered adsorbed layers. Is it possible to characterize the type and amount of disorder from the vibrational properties? To answer this question, we are currently exploring the lattice dynamics of binary mixtures of the rare gases in the monolayer and bilayer regime. Preliminary results indicate that there is a difference between the phonon dispersion of the completely mixed Ar-Kr bilayer as compared to the bilayer system consisting of a Kr monolayer adsorbed on top of a pure Ar monolayer on Pt(111). These differences may be accounted

for by interlayer stress or structural disorder. Very exciting experimental results have been reported recently on the vibrational properties of fractal structures[31]; in addition, a theoretical study by Black[32] discusses the dynamic behavior of fractally ordered 2D adlayers.

Finally, a completely different area of application of energy resolved spectroscopy is the study of kinetic processes, such as surface diffusion. In recent years considerable progress has been achieved in characterizing the mobility and the diffusion in disordered or premolten films. For this purpose the inelastic lineshape of the incoherent elastic scattering signal is measured, and the mobility of the diffusing atoms is extracted from the Doppler-like "quasi-elastic" broadening of the incoherent elastic peak. Since this broadening is typically very small, most of the experimental studies have so far been carried out using *Q*uasi-*E*lastic *N*eutron *S*cattering (QUENS)[33] where the required energy resolution $< 100\ \mu eV$ is easily obtained. The first quasielastic He scattering study on a Pb(110) surface has been reported recently[34], showing that surface kinetics on single crystal surfaces and adsorbed layers can also be accessed with He scattering.

Since many of the possible applications mentioned above have not yet been explored in detail, vibrational spectroscopy as a surface investigation tool for the understanding of physisorption systems and thin films will continue to be a fascinating and tempting field.

7. REFERENCES

1. A. Thomy and X. Duval, J. Chim. Phys. 67 (1970) 1101; for an overview see: R. Marx, Physics Reports 1 (1985) 1
2. A. Thomy, X. Duval, and J. Reignier, Surf. Sci. Rep. 1 (1981) 1
3. M. D. Chinn, S. C. Fain, and R. D. Diehl, Phys. Rev. B21 (1980) 4170; D. E. Moncton, P. W. Stephens, R. J. Birgeneau, P.M. Horn, and G. S. Brown, Phys. Rev. Lett. 46 (1980) 1533
4. E. D. Specht, A. Mak, C. Peters, M. Sutton, R. J. Birgeneau, K. L. D'Amico, D. E. Moncton, S. E. Nagler, and P. M. Horn, Z. Physik B69 (1987) 347; J. Cui, S. C. Fain, H. Freimuth, H. Wiechert, H. P. Schildberg, and H. J. Lauter, Phys. Rev. Lett. 60 (1988) 1848 K. Kern, P. Zeppenfeld, R. David, and G. Comsa, J. Vac. Sci. Technol. A6 (1988) 639
5. W. A. Steele, Surf. Sci. 36 (1973) 317
6. R. Pandit, M. Schick, and M. Wortis, Phys. Rev. B29 (1982) 5112
7. P. Bak, in Chemistry and Physics of Solid Surfaces V, ed. by R. Vanselow and R. Howe, Springer, Berlin, 1984, p. 317
8. B. F. Mason and B. R. Williams, Phys. Rev. Lett. 46 (1981) 1138
9. K. D. Gibson and S. J. Sibener, Faraday Discuss. Chem. Soc. 80 (1985) 203 and Phys. Rev. Lett. 55 (1985) 514; K. D. Gibson, S. J. Sibener, B. M. Hall, D. L. Mills, and J. E. Black, J. Chem. Phys. 83 (1985) 4256
10. K. Kern, R. David, R. L. Palmer, and G. Comsa, Phys. Rev. Lett. 56 (1986) 2823
11. B. M. Hall, D. L. Mills, and J. E. Black, Phys. Rev. B32 (1985) 4932

12. K. Kern, P. Zeppenfeld, R. David, and G. Comsa, Phys. Rev. B35 (1987) 886 and J. Electr. Spectr. Relat. Phenom. 44 (1987) 215
13. B. M. Hall, D. L. Mills, P. Zeppenfeld, K. Kern, U. Becher, and G. Comsa, Phys. Rev. B40 (1989) 6326
14. P. Zeppenfeld, U. Becher, K. Kern, R. David, and G. Comsa, Phys. Rev. B41 (1990) 8549
15. K. Kern, U. Becher, P. Zeppenfeld, G. Comsa, B. M. Hall, and D. L. Mills, Chem. Phys. Lett. 167 (1990) 362
16. I. Estermann and O. Stern, Z. Physik 61 (1930) 95
17. A. Kantrowitz and J. Grey, Rev. Sci. Instrum. 22 (1951) 328; J. B. Anderson and J. B. Fenn, Phys. Fluids 8 (1965) 780
18. B. Poelsema and G. Comsa, Springer Tracts in Modern Physics Vol. 115, Springer, Berlin, 1989
19. T. Engel and K. H. Rieder, Springer Tracts in Modern Physics Vol. 92, Springer, Berlin, 1982
20. J. P. Toennies, J. Vac. Sci. Technol. A5 (1987) 440; K. Kern and G. Comsa, Adv. Chem. Phys. 76 (1989) 211
21. R. David, K. Kern, P. Zeppenfeld, and G. Comsa, Rev. Sci. Instrum. 57 (1986) 2771
22. L. K. Verheij and P. Zeppenfeld, Rev. Sci. Instrum. 58 (1987) 2138 and references therein
23. U. Linke and B. Poelsema, J. Phys. E 18 (1985) 26
24. E. de Rouffignac, G. P. Alldredge, and F. W. de Wette, Phys. Rev. B24 (1981) 6050
25. K. D. Gibson, S. J. Sibener, B. M. Hall, D. L. Mills, and J. E. Black, J. Chem . Phys. 83 (1989) 4256
26. J. P. Toennies and R. Vollmer, Phys. Rev. B40 (1989) 3495
27. K. Kern, R. David, R. L. Palmer, G. Comsa, and T. S. Rahman, Phys. Rev. B33 (1986) 4334; V. Bortolani, A. Franchini, G. Santoro, J. P. Toennies, Ch. Wöll, and G. Zhang, ibid. 40 (1989) 3524
28. H. Ibach and D. L. Mills, Electron Energy Loss Spectroscopy and surface vibrations, Academic Press, 1982
29. H. Taub, L. Passell, J. K. Kjems, K. Garneiro, J. P. McTague, and J. G. Dash, Phys. Rev. Lett. 34 (1975) 654
30. V. L. P. Frank, H. J. Lauter, and P. Leiderer, Phys. Rev. Lett. 61 (1988) 436
31. E. Courtens, J. Pelous, R. Vacher, and T. Woignier, Phys. Rev. Lett. 58 (1987) 128; R. Vacher, T. Woignier, J. Pelous, G. Coddens, and E. Courtens, Europhys. Lett. 8 (1989) 161
32. J. E. Black, Phys. Rev. B38 (1988) 2151
33. M. Bienfait, Europhys. Lett. 4 (1987) 79; M. Bienfait, P. Zeppenfeld, J. M. Gay, and J. P. Palmari, Surf. Sci. 226 (1990) 327
34. J. W. M. Frenken, J. P. Toennies, and Ch. Wöll, Phys. Rev. Lett. 60, 1727 (1988); J. W. M. Frenken, B. J. Hinch, and J. P. Toennies, Surf. Sci. 211/212 (1989) 21